Supporting Information

Leaf-Like Hematite-Decorated Flexible Carbon-Textile for Enhancing Mass Transfer at Triphasic Interfaces in Photoanodes

Zhou Zhou[a, #], *Mengmeng Zhu*[a, #], *Chengkun Song*[a, b, #], *Mingyu Tang*[a], *Shujing Li*[a], *Xiangyu Meng*[a, b, *], *Yueming Sun*[a], *Yunqian Dai*[a, b, *]

[a] School of Chemistry and Chemical Engineering, Southeast University, Nanjing, Jiangsu 211189, P. R. China

[b] Purple Mountain Laboratories, Nanjing, Jiangsu 211111, P. R. China

[#] These authors contributed equally to this work.

[*] Corresponding author: daiy@seu.edu.cn, xiangyu.meng@seu.edu.cn

Fig. S1 Optical images of cotton cloth and carbon cloth.

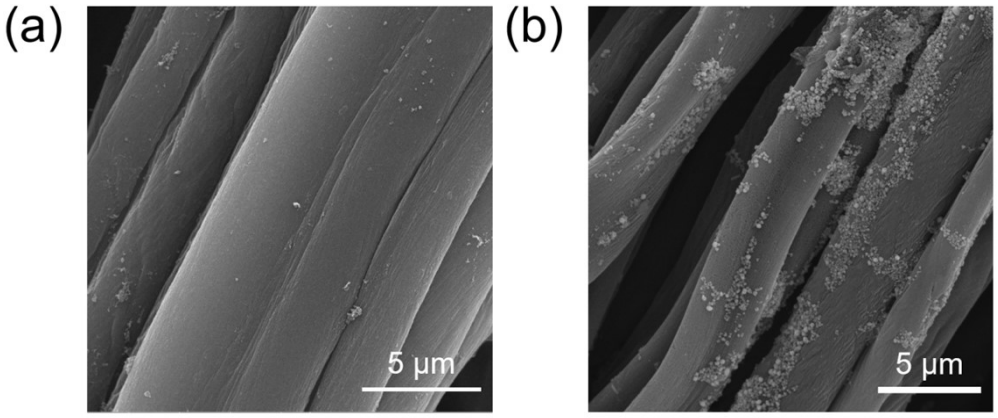

Fig. S2 SEM of (**a**) Unoxidized carbon cloth has a smooth surface (**b**) Unoxidized carbon cloth loaded with α-Fe_2O_3.

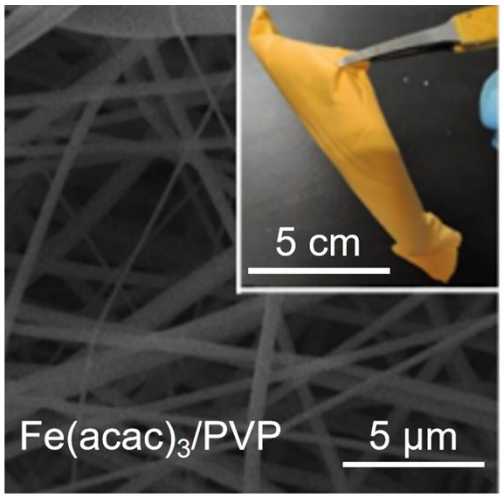

Fig. S3 SEM image and optical image of $Fe(acac)_3$/PVP nanofibers. The inset is the optical image of $Fe(acac)_3$/PVP fibrous mat.

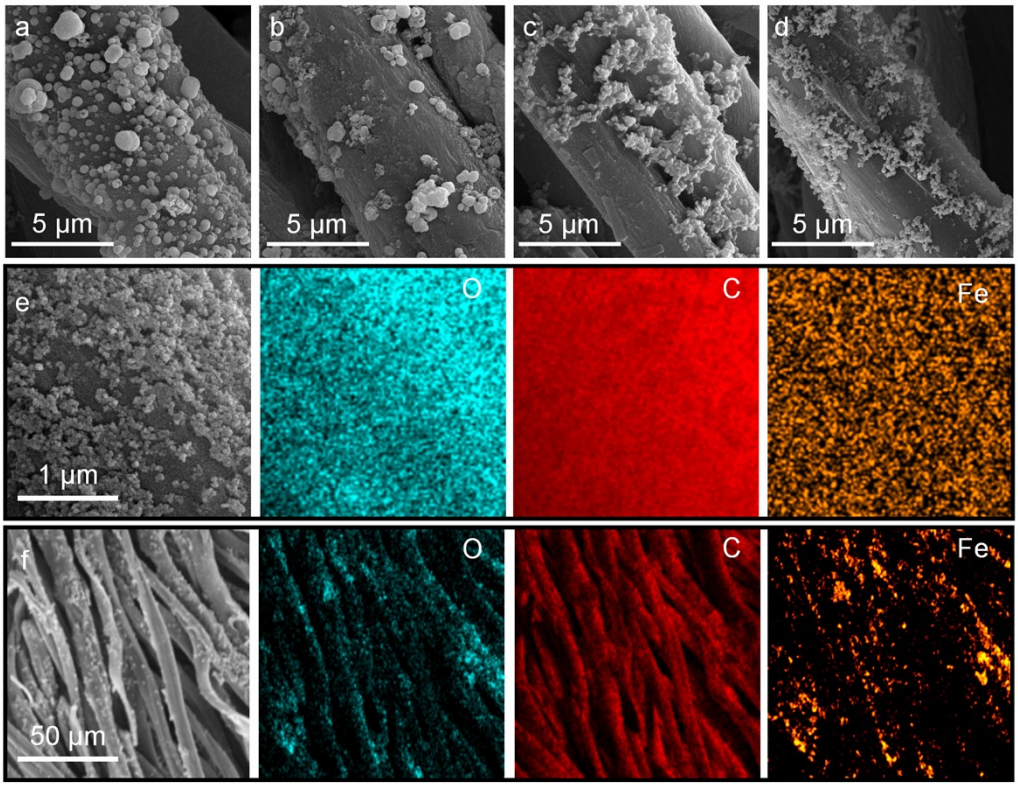

Fig. S4 (**a**–**d**) SEM images of carbon oxide cloth hydrothermally loaded with Fe_2O_3 for 2 h, 4 h, 6 h, 8 h. (**e, f**) The SEM image of α-Fe_2O_3@oxidized carbon cloth-64 is listed in the first column, and the rest is the EDS image of α-Fe_2O_3@oxidized carbon cloth-64.

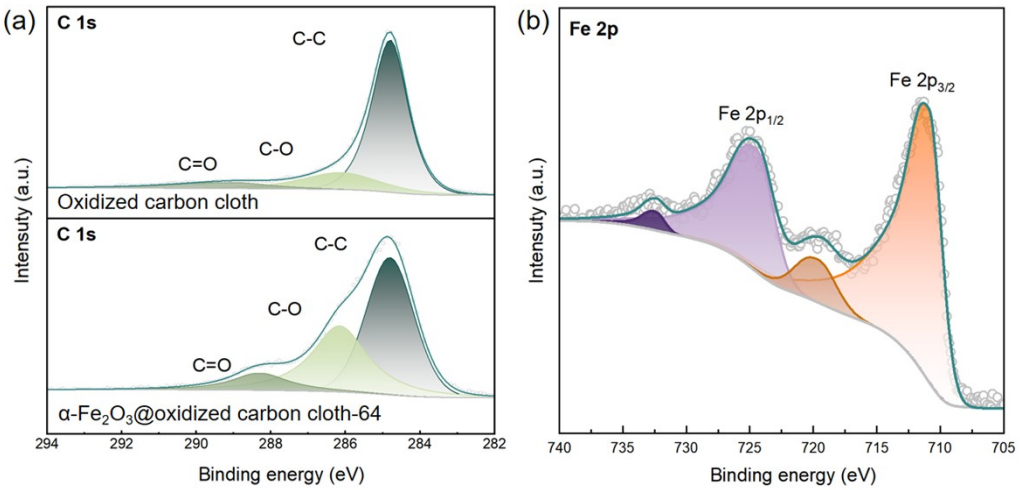

Fig. S5 XPS spectra of (**a**) C 1*s* of oxidized carbon cloth and α-Fe_2O_3@oxidized carbon cloth-64, (**b**) Fe 2*p* of α-Fe_2O_3@oxidized carbon cloth-64.

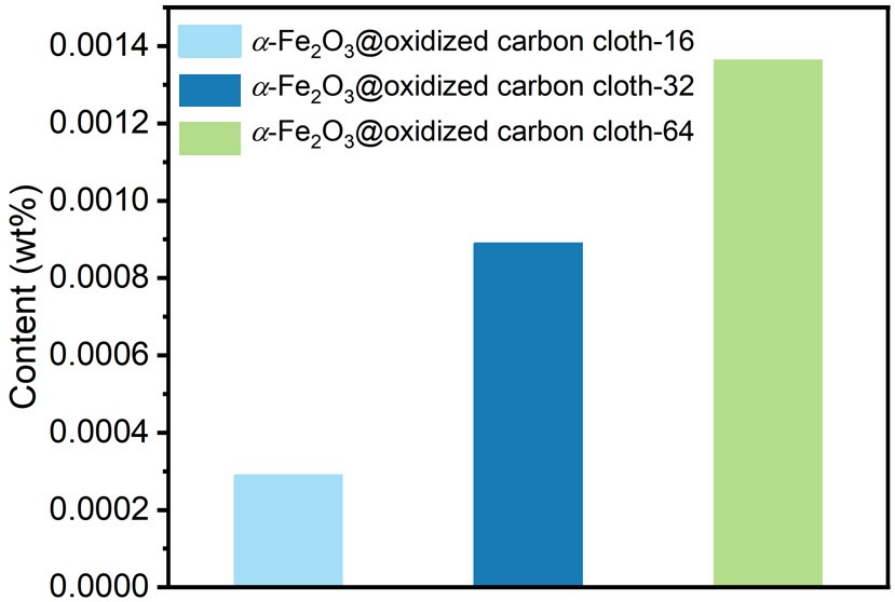

Fig. S6 ICP-MS of α-Fe_2O_3@oxidized carbon cloth-16, 32, 64. The ordinate is the content of Fe element per mg of oxidized carbon cloth.

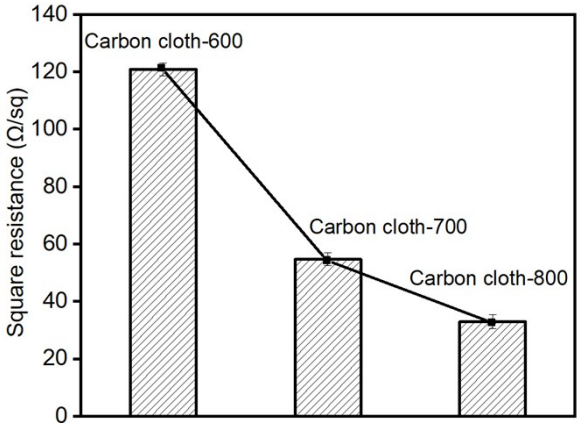

Fig. S7 Surface resistance of carbon with different carbonization temperatures.

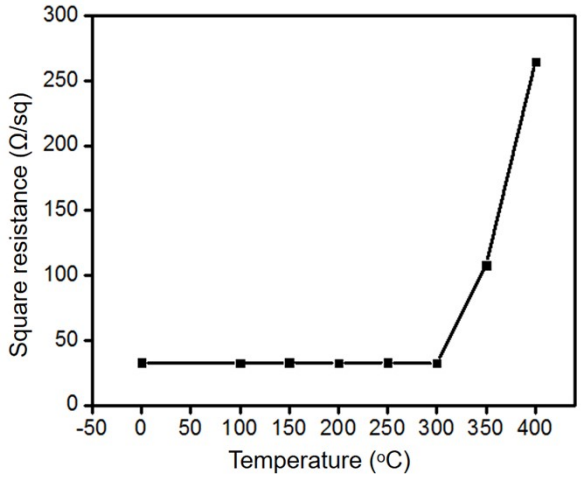

Fig. S8 The influence of different thermal oxidation temperatures on the resistance of carbon cloth-800.

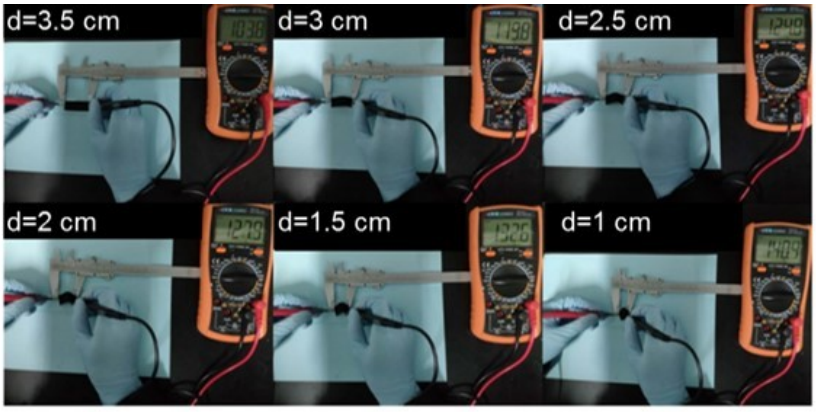

Fig. S9 The resistance changes of carbon cloth-800 under different curvature deformations.

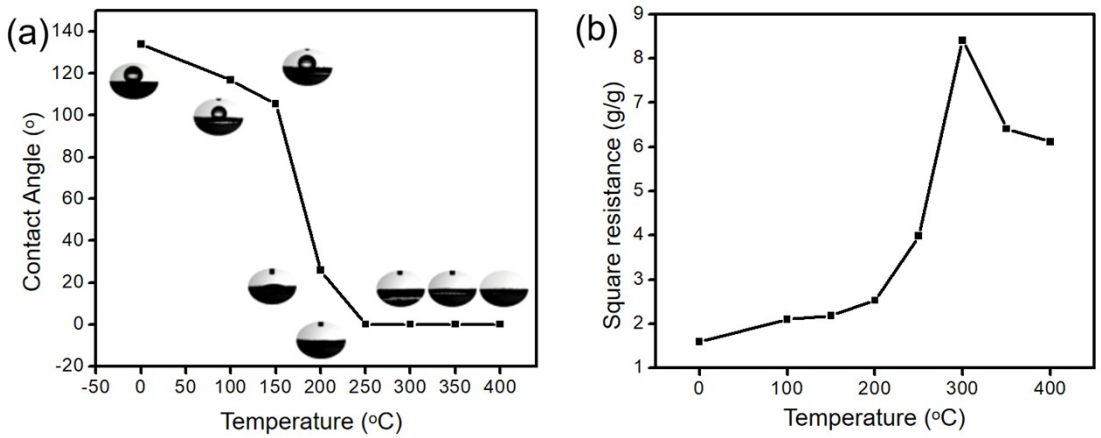

Fig. S10 The influence of the contact angle (**a**) and the liquid absorption rate (**b**) of the carbon cloth-800 surface at different thermal oxidation temperatures.

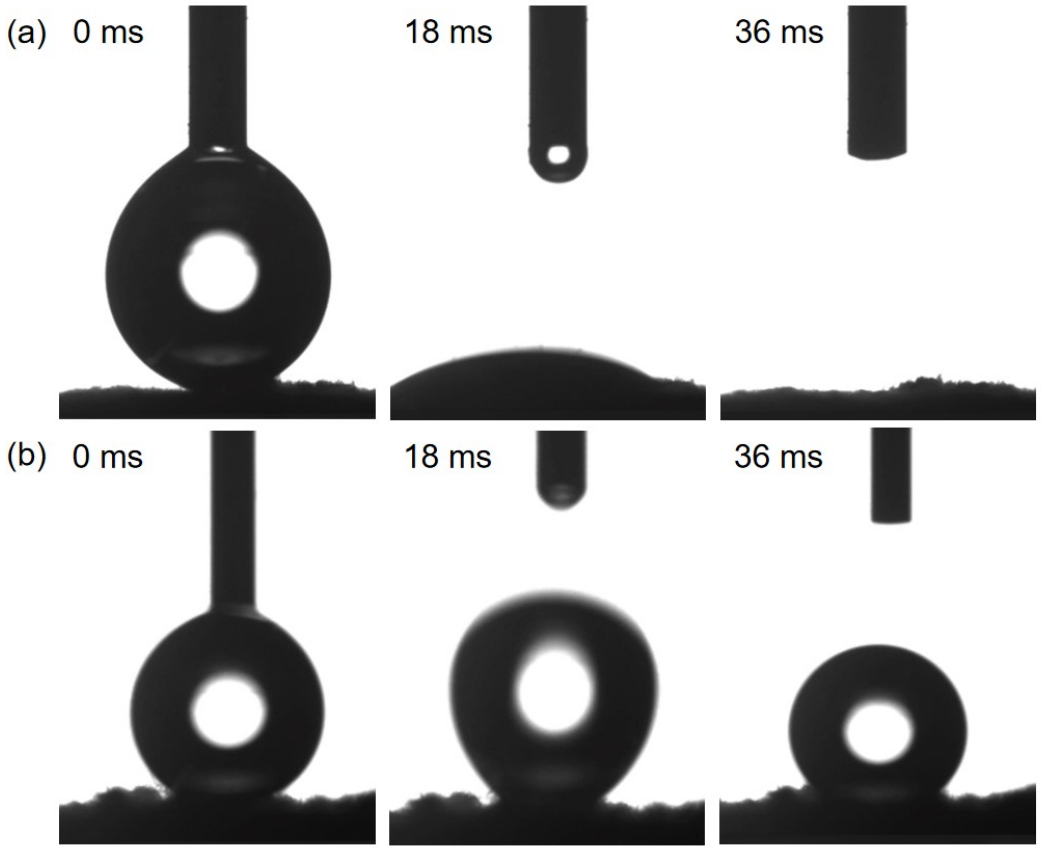

Fig. S11 Water contact angle of (**a**) oxidized carbon cloth and (**b**) carbon cloth.

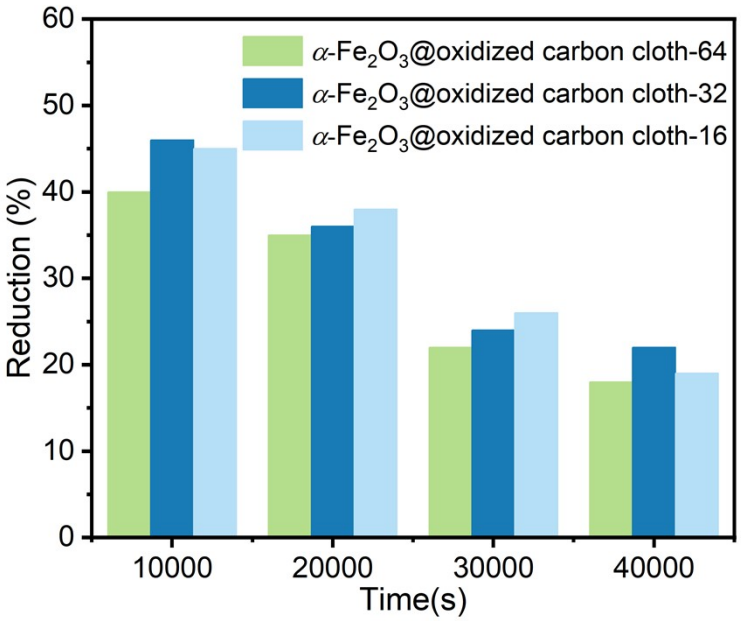

Fig. S12 The percentage of current reduction per 10000 s of α-Fe_2O_3@oxidized carbon cloth-16, 32, 64.

Table S1. The EIS results for α-Fe_2O_3@oxidized carbon cloth-16, 32, 64.

Materials	α-Fe_2O_3@oxidized carbon cloth-16	α-Fe_2O_3@oxidized carbon cloth-32	α-Fe_2O_3@oxidized carbon cloth-64
CTR1/Ω	89.4	97.3	54.1
CTR2/Ω	310.3	292	319.4

Table S2 Comparison of this work with other advanced work.

Photoelectrode	Methods	Electrolyte	Current density ($mA \cdot cm^{-2}$)	Overpotential (mV)	Tafel plots ($mV \cdot dec^{-1}$)	Ref.
α-Fe_2O_3@oxidized carbon cloth-64	Electrospinning, Hydrothermal	H_2SO_4	10	193	42	This work
Er-RuO_x	Electrospinning, Pyrolysis	H_2SO_4	10	200	45	40
Ir^{VI}-ado	Oxidative ligand substitution, Electrodeposition	H_2SO_4	10	250	32	41
Ta-RuO_2	Molten salt method	$HClO_4$	10	201	55	42
$Ni(OH)_2$/NF	Electroplating	KOH	10	200	52.6	43
CuCo Diatomic Catalysts	Ball-Milling, Pyrolysis	KOH	10	339	45.3	44
Irw-Co_3O_4@NC	Ir doping via ion exchange, Pyrolysis	KOH	10	244	60	45
$LaMnO_3$(LMNO)	Nitridation	KOH	10	250	54	46
NiBDC-FcCA	Solvothermal reaction	KOH	10	280	46.3	47
$Ni_{0.75}Fe_{0.25}O_x$(001)	Magnetron sputtering	KOH	10	289	48	48
NP-$(FeCoNi)_2Nb$	Melt-spinning, Chemical dealloying	KOH	10	235	63.6	49
Ni_2P-NCDs-$Co(OH)_2$-NF-3	Immersion	KOH	500	389	65	50
CeO_2/CoS_2-6	Hydrothermal	KOH	10	283	33.2	51
Co/CoO_x/NCNFs-0.1	Electrospinning, Annealing	KOH	10	429	109.4	52